Daric Fitzwater
Department of Mechanical Engineering,
IUPUI,
Indianapolis, IN 46202
e-mail: defitzwa@iupui.edu

Todd Dodge
Department of Biomedical Engineering,
IUPUI,
Indianapolis, IN 46202
e-mail: trdodge@iupui.edu

Stanley Chien
Department of Electrical Engineering,
IUPUI,
Indianapolis, IN 46202
e-mail: schien@iupui.edu

Hiroki Yokota
Department of Biomedical Engineering,
IUPUI,
Indianapolis, IN 46202
e-mail: hyokota@iupui.edu

Sohel Anwar
Department of Mechanical Engineering,
IUPUI,
Indianapolis, IN 46202
e-mail: soanwar@iupui.edu

Development of a Portable Knee Rehabilitation Device That Uses Mechanical Loading

Joint loading is a recently developed mechanical modality, which potentially provides a therapeutic regimen to activate bone formation and prevent degradation of joint tissues. To our knowledge, however, few joint loading devices are available for clinical or point-of-care applications. Using a voice-coil actuator, we developed an electromechanical loading system appropriate for human studies and preclinical trials that should prove both safe and effective. Two specific tasks for this loading system were development of loading conditions (magnitude and frequency) suitable for humans, and provision of a convenient and portable joint loading apparatus. Desktop devices have been previously designed to evaluate the effects of various loading conditions using small and large animals. However, a portable knee loading device is more desirable from a usability point of view. In this paper, we present such a device that is designed to be portable, providing a compact, user-friendly loader. The portable device was employed to evaluate its capabilities using a human knee model. The portable device was characterized for force-pulse width modulation duty cycle and loading frequency properties. The results demonstrate that the device is capable of producing the necessary magnitude of forces at appropriate frequencies to promote the stimulation of bone growth and which can be used in clinical studies for further evaluations. [DOI: 10.1115/1.4024830]

Introduction

Controlled knee loading has been shown to provide therapeutic and stimulating effects on the long bones found in the hind limbs [1]. While loading of the knee joint has not previously been tested in clinical trials, numerous animal studies have demonstrated the potential therapeutic effects of this treatment modality. Dynamic loads applied laterally to the knee joint have been found to stimulate new bone formation not only in the distal femur and proximal tibia epiphyses, but along the entire length of each bone. The loading force required to stimulate bone formation due to knee loading is lower than that of other mechanical loading regimens, and strains in areas of bone formation are also reduced [2]. This characteristic makes knee loading an attractive potential treatment in accelerating fracture repair, and many studies have been conducted to investigate its effects. Using surgical holes to simulate bone fractures in the tibia diaphysis, knee loading has been shown to accelerate fracture healing while maintaining small mechanical strain at the fracture site [3]. Knee loading has also reduced healing time in wounds far from the loading site in animal studies. Fractures of the femoral neck, which are a serious public health concern, experience faster healing times as a result of dynamic knee loading. To explain the observed increases in bone formation due to knee loading, studies have focused on biophysical and molecular mechanisms that occur during and following a loading treatment. Knee loading is applied laterally to the epiphysis of the femur and tibia, which consist mostly of trabecular bone modeled to resist axial stresses. This allows greater deformations than are possible with similar loads in different loading modalities. Dynamic deformations of the epiphysis cause alterations in fluid pressure in the intramedullary cavity, driving oscillatory fluid flow and molecular transport in the lacunocanalicular network in the bone matrix and in the medullary cavity [4–6]. Fluid flow may cause shear stress to osteocytes, stimulating a Wnt-signaling pathway, leading to osteoblast differentiation and the initiation of bone formation [7]. The results from animal studies demonstrate the potential therapeutic effects of knee loading in diseases of low bone mass, in cases of disuse, and in bone fracture treatment.

This paper shows the design and testing of such a portable device proposed to implement controlled knee loading on humans. The device applies cyclic loading of magnitudes up to 30 N at frequencies ranging from 1 to 20 Hz and can cause small deformation in the knee. The device faces several constraints such as voltage, space, mass, force, and frequency limits for both functional and safety reasons. There are also a number of design considerations to address concerning the mechanical behavior. Since the device will be used in testing situations where precise force and frequency applications are essential, damping and deformation must be minimized as the damping caused by bending and deformation of the device components could alter measurements and lead to inaccurate calibration and application of the device.

Several devices have been produced and marketed as bone stimulating devices for restorative purposes. These devices use several different principals to accomplish bone cell stimulation. One device currently used and representing ultrasonic vibrators is the Exogen 2000+. The Exogen 2000+ wraps around a limb and vibrates the fluid within to accomplish stimulation [8]. Another device, the Physio-Stim Lite, uses electromagnetic field pulses to induce small electric fields in bone tissue in order to stimulate the bone tissue by inducing low-magnitude and high-frequency loading of the bone tissue [9]. These devices and others of similar operation have found use in some medical cases for use in therapy [10,11].

The device proposed in this paper differs in that it stimulates the bone tissue through direct mechanical loading at low frequencies. Operating the device at frequencies between 1 and 5 Hz is meant to simulate the therapeutic and rehabilitative effects of walking or running without the need to put the patient's weight on the leg. This makes the device an ideal candidate for speeding the recovery of fractures or combating the progress of bone degenerative diseases, such as osteoporosis and arthritis where the mobility

Manuscript received August 9, 2012; final manuscript received May 2, 2013; published online September 24, 2013. Assoc. Editor: Jahangir Rastegar.

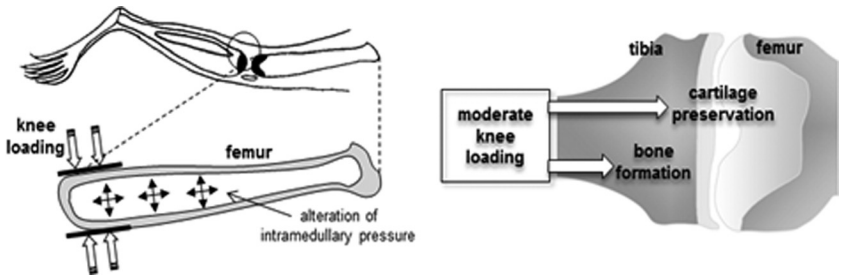

Fig. 1 (*a*) Depiction of fluid flow, pressure, and deformation within a bone, and (*b*) mechanical loading of a knee joint

of patients is limited. Since it operates at such low frequencies, there is little concern for development of vibration syndrome after prolonged use.

Previous Studies

The healing process of long bones can be stimulated by mechanical means. This stimulation of the bone tissue is caused by the rhythmic movement of fluid along the length of the bone and the resulting internal pressures and displacements [1]. The enhanced bone growth caused by such tissue stimulation can enhance the healing speed of fractures within the bone as well as increase the density of the bone, something that could prove useful in the prevention or even treatment of osteoporosis. Several areas of research have opened within the field of biomedical engineering relating to the purposeful stimulation of bone growth. Figure 1 depicts the working hypothesis of fluid movement within a bone and mechanical loading of a bone.

To apply such a load, a device would need to have a means of producing a transverse force directly to the end of a long bone, such as at the knee. A cyclic force applied on such an area would force a slight shift of the fluid within the bone towards the opposite end of the bone in a controlled fashion. While no such device currently exists for use on humans, a new interdisciplinary study in our research group seeks to develop a portable device designed for humans; the proposed device will be used in future testing. While such a device has not been used for humans prior to this paper, research has been performed in the past using various animals and similar devices for animals while trying to determine the degree of effectiveness of such treatment. Figure 2 shows a table-top type device that was used to load the knee of rats and small pigs. These devices were shown to be effective in inducing new bone tissue. Further details and research can be found in Refs. [5–7].

Fig. 2 Table setup version of a knee-loading device used for testing the knee of a rat

Design

The device was designed to provide a portable means of safely loading a human knee with the goal of stimulating increased bone tissue growth. This goal introduced several challenges that required a careful design to overcome. The device must provide sufficient force in a transverse load to the joint without being bulky or unbalanced. The device must be sufficiently light as to be easily mobile. The device must have some form of control that allows for selection of specific run times, frequencies, and forces. For the sake of mobility, the control must also be easily transported with the device.

Design Process and Constraints. Various constraints are present when making such a device. To quantify these constraints, certain concrete targets were set to help refine the decision making process. Firstly, the device must run at a relatively low voltage for safety reasons, preferably less than 25 V. Next, the device must be adjustable, allowing at least a variance of 5 cm in the components holding the knee to accommodate varying knee diameters. The device has to be compact, with the mechanical components taking up no more than a (30 cm × 30 cm × 15 cm) space for easy storage in a transportable case. The device should be lightweight, weighing no more than 4 kg with less being always preferred. The device must be capable of producing a range of forces to be useful in future research, not just fixed force magnitudes. The force magnitudes that the device can produce must be at least 30 N. The device must be capable of running at any frequency between 1 and 5 Hz. Lastly, the device was required to have a degree of user friendliness. This constraint was not easily quantifiable, thus concepts were evaluated relative to each other for this constraint. In order to better analyze concepts and consider more options, the design of the device was broken down into functional categories: containment, power source, force generation, force transfer, and control. Bearing the listed constraints in mind, a number of possible solutions were proposed for each major function of the device. Note that not all functional areas of the device were found to affect every constraint.

The function of containment is the part of the device that provides the structure and attachment points for all other functional components. It can be either hard or soft, with a number of possible solutions. The concepts evaluated for this device were a rigid metal frame, a flexible cast, a rigid cast, and a flexible cloth brace.

The power source is what provides the energy for the operation of the device. The design team identified two key options for this function. Concepts that were considered were batteries and a wall outlet.

As mentioned in the previous section, this device had several preceding prototypes and similar devices used for animal testing. These were used as benchmarks and references to the various ideas that were proposed. From these, it was found that the voice coil motor was capable of satisfying many of the requirement and constraints, so this motor was again considered. Other power sources that were also considered were an electric brushed dc motor, a

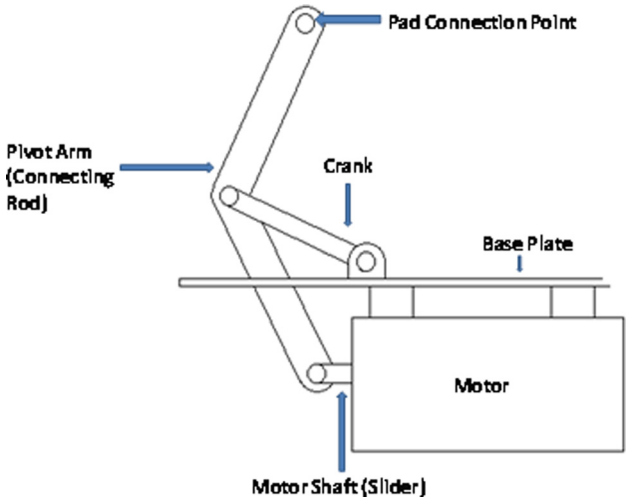

Fig. 3 Diagram of proposed mechanism

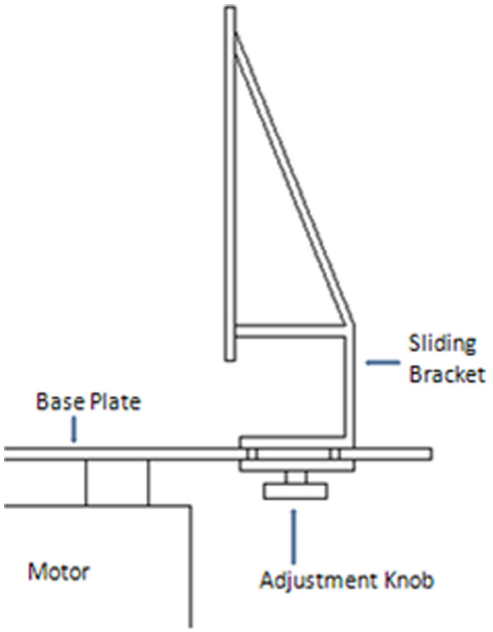

Fig. 4 Adjustable side using contact resistance

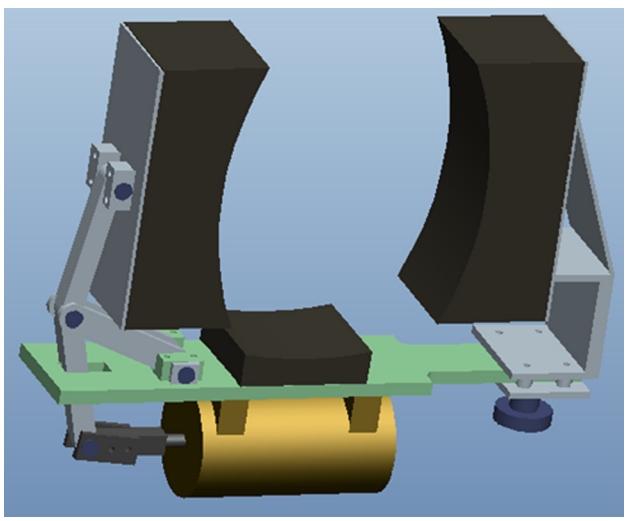

Fig. 5 Pro/Engineer solid model of device

piezoelectric motor, an air pump with a piston, and electroactive polymers.

In the past prototypes and research devices, direct force transmission was most frequently used. However, it was found from these prototypes and previous devices used in animal testing that a motor alone was hard to incorporate into a compact and a well-balanced design. Thus, power generation units used in conjunction with a mechanism comprised of linkages was proposed as a means of shifting the power generation component into a position that allowed for better balance. Other means of accomplishing efficient force transmission that were also considered were gears, a transfer fluid, and a cam.

Several means of control were also proposed. Regardless of the means, it was decided that the control module for the device must be user friendly, allow for a range of forces and frequencies, and be portable with the device. Because of this last requirement, emphasis was placed on a means of standalone control that did not require connection to a PC. Two primary concepts were evaluated, a timer/amplifier circuit similar to that used in a previous prototype and a microcontroller and amplifier circuit combination.

From the evaluation of various possible solutions, it was decided that the final design would use a voice coil motor with a mechanism that allowed low voltage, easy adjustment, a compact design, variable force, and a range of forces that included the target range. A metal frame was used for the structural support of the device. AC power from a standard wall outlet was used via an adaptor. A microcontroller was used to control the device as it provided a means to add a simple user interface.

Mechanism Design. The mechanism used for the loading device was purposefully made as simple as possible while still approximating linear movement. It is functionally a type of offset crank-slider mechanism but with the apex of the connecting rod being the output instead of the slider or crank. For this setup, the motor shaft is acting as the sliding block while the linkage connecting to the base plate serves as the crank. The rigid pivot arm that connects the motor shaft and crank before ultimately connecting with the pad at the top is the connecting arm. This is shown in Fig. 3.

The device must also accommodate a range of knee sizes to be useful. This necessitates an adjustable side plate on the opposite side with the linkage that can be used to control the distance between the plates, the gap where the knee rests. The proposed design is for a sliding bracket which pinches the base plate between two contact surfaces. These surfaces are loose enough to allow easy sliding over the base plate. However, when a knob is used to turn a short bolt, the surfaces are pressed together tightly, arresting movement. A diagram of this concept is shown in Fig. 4.

Several motors were considered for this device, but ultimately a moving magnet voice coil motor was selected as it provides linear movement with a swift response time and forces within the desired range of 0–30 N. The exact motor chosen was the NCM03-20-089-2LB (Non-Comm Moving Magnet Actuator H2W Technologies Inc.), capable of operating from low to mid frequencies and providing up to 39.6 N of continuous force. Once the dimensions of the motor were obtained, a dimensioned design could be made using the solid modeling software Pro/Engineer developed by PTC whose main headquarters is in Needham, MA. The as-built solid model is shown in Fig. 5.

The range of linear motion that the motor provides is 6.35 mm. This should correspond to a roughly equal or slightly greater amount of motion in the side plate that presses against the knee, but not a lesser amount. Since a linkage with pin joints is used as

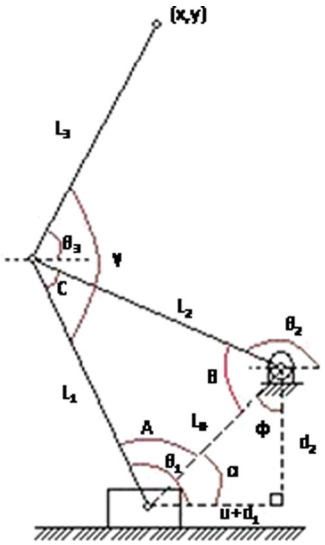

Fig. 6 Simplified representation of the slider crank mechanism used for the force transmission in the device

the mechanism, the movement will be a linear approximation. The linkage can be mathematically modeled with several equations. These equations will refer to the nomenclature used in the simplified representation of the linkage shown in Fig. 6.

For this application, the lengths d_1, d_2, L_1, L_2, L_3, and γ are known. The position of the point (x,y) is the output. For this setup, u is the distance the motor shaft is extended and is the input. The position of point (x,y) can be calculated analytically using vector equations and the law of cosines. The first step in this process is to calculate the value of L_0. This is given by Eq. (1),

$$L_0 = \sqrt{(u + d_1)^2 + d_2^2} \tag{1}$$

Using this and the known constants, the angles φ and α can be calculated using the definition of cosine

$$\varphi = \cos^{-1}\left(\frac{d_2}{L_0}\right) \tag{2}$$

$$\alpha = 90\,\text{deg} - \varphi \tag{3}$$

Using the law of cosines, the angles A and B can be calculated. These are given in Eqs. (4) and (5),

$$A = \cos^{-1}\left(\frac{L_0^2 + L_1^2 - L_2^2}{2L_0L_1}\right) \tag{4}$$

$$B = \cos^{-1}\left(\frac{L_0^2 + L_2^2 - L_1^2}{2L_0L_2}\right) \tag{5}$$

Using angles A and B, angles θ_2 and θ_3 can be easily calculated. These expressions are shown in Eqs. (6) and (7),

$$\theta_2 = 270\,\text{deg} - \varphi - B \tag{6}$$

$$\theta_3 = A + \alpha + \gamma - 180\,\text{deg} \tag{7}$$

The position of the x and y coordinates of point (x,y) can be calculated using the vector equations shown in Eqs. (8) and (9),

$$x = L_2 \cos\theta_2 + L_3 \cos\theta_3 \tag{8}$$

$$y = L_2 \sin\theta_2 + L_3 \sin\theta_3 \tag{9}$$

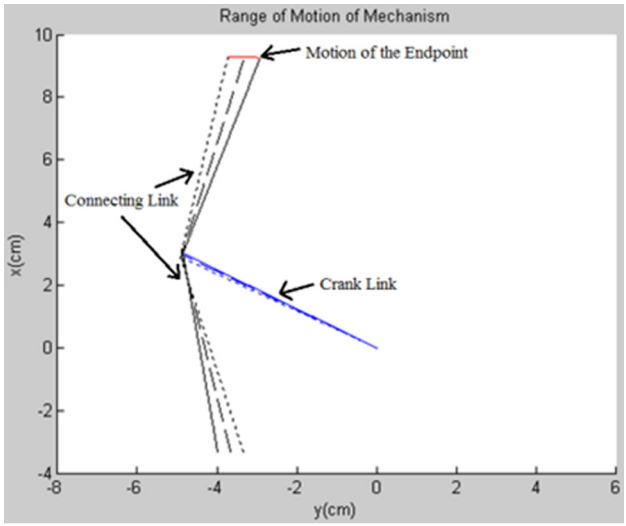

(a)

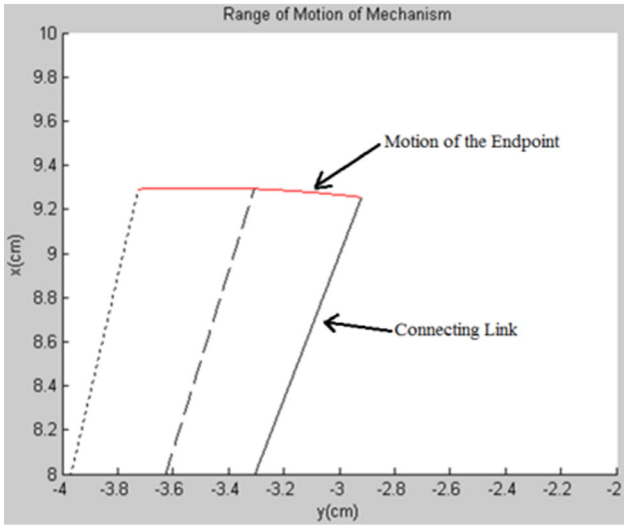

(b)

Fig. 7 (*a*) The top curve shows the motion of the end point of the connecting rod through the *x–y* plane; the long solid lines (vertically aligned and diagonally aligned) show three positions of the connecting and crank links, respectively. (*b*) Motion of the end point of the connection rod showing its linear approximation.

Substituting the values calculated in Eqs. (1)–(7), x and y can be calculated for any value of u. A program was made in MATLAB 2010, a high-level language for computation developed by MathWorks based in Natick, MA, to calculate the values of x and y for values of u between 0 and 6.35 mm. The code then creates a figure displaying the motion in the x–y plane and provides the range of motion along the horizontal. From this program, it was calculated that for the max motor displacement of 6.35 mm the lever arm moved 8.07 mm along the horizontal, which provides an improved adjustable range for overcoming the displacement of the soft tissue on the sides of the knee. Figure 7 shows the motion of point (x,y) as a red line. The lever arm and crank are shown in three different positions in black and blue, respectively. As can be seen in the figure, the motion of point (x,y) is not perfectly linear, but makes a fair approximation for this range of motion. Further information on mechanics of mechanisms can be found in Ref. [12].

Material Selection. The materials for the final design were selected to achieve both strength and minimal weight. Aluminum

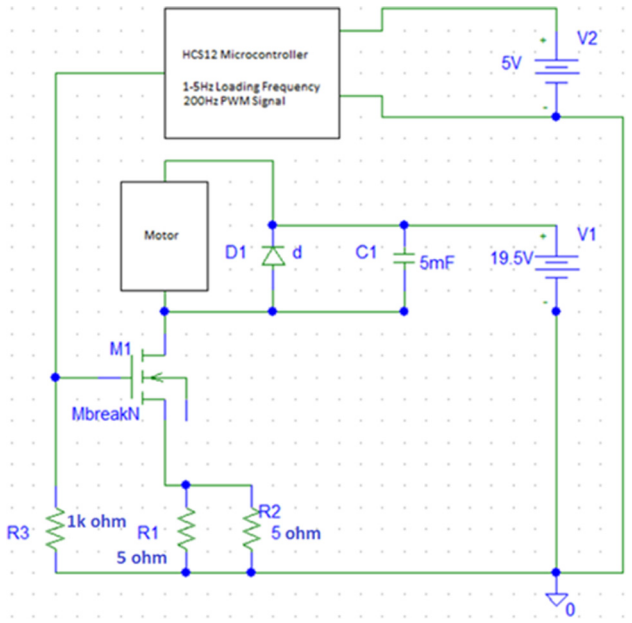

Fig. 8 Circuit design for the device control module

was chosen for the base plate, side plates, and the adjustable side as it is lightweight, but still provides the necessary strength. The pivot arm and lever arm were made of O1 steel. O1 steel has a high carbon content and a correspondingly high modulus of elasticity. This is crucial as these parts are subjected to higher stresses than are found in any other part of the device; it is important to minimize the deflection in these pieces since deflection of these parts would directly affect the range of displacement provided by the mechanism and may also contribute to damping. High density polyethylene was selected for the pads as it allows a slight amount of deformation to increase comfort to the user while still being sufficiently rigid to transfer most of the force to the knee being loaded.

Circuit Design. A microcontroller with an amplifier circuit was used to drive the voice coil actuator [15]. The microcontroller is powered by a 5 V supply; the amplifying circuit is powered by a 19.5 V supply. The voltage supplies share a common ground. The output force of the motor is proportional to the input voltage, which is proportional to the duty cycle of the PWM signal produced by the controller. The PWM signal is turned on and off to produce the loading frequency. The maximum amplitude of the PWM signal produced by the controller is 5 V. This signal is amplified by an enhancement type MOSFET. A 1000 Ω resistor (R3) connects the MOSFET gate to the ground to set the bias voltage. The motor is in parallel with a 5 mF capacitor to smooth the operation and reduce noise. The circuit layout is shown in the diagram in Fig. 8.

Programming Architecture. The HCS12 microcontroller used for the device was programmed using assembly language [13, 14]. The inputs to the controller were five push buttons while the output was a pulse width modulation signal and an LCD display. Upon startup, the controller requests the user to enter the desired force, loading frequency, and run time. Push buttons are used to scroll down the rows and increase or decrease the settings of each option. The force can be set between 5% and 100% duty cycles of the motor (see the section on Test Results for corresponding values in N) with a step increment of 5%. The frequency setting is allowed to range between 0 and 20 Hz with a step increment of 1 Hz; the 0 Hz setting corresponds to a constant load which can be used during calibration. The run time can range from 30 s to 30 min with a step increment of 30 s.

Once all settings are entered and the execute button is pressed, the controller runs checks to ensure that the settings are within the acceptable ranges. If a setting is not within the predefined range, the program will branch back to the input screen requesting a new value. If all settings are accepted, the program initializes the remaining variables and waits for the user to press the execute button. Once the execute button is pressed, the controller enters the run loop and begins sending the loading signal to the amplifier circuit and the device will run for its allotted time. The screen will show the current settings and operational time remaining during the run loop. The execute command can be pressed at any time to pause the device and pressed again to unpause; the check for the button press is made within the run loop. The reset button can be pressed at any time for any phase of operation to turn off the device and restart the program through the use of a dedicated interrupt.

As-Built Device. The device was constructed; the material of the mechanical structure is aluminum, the pads are high density polyethylene, and the linkage mechanism is steel. The controller and amplifier circuit were enclosed in a plastic controller box. The device is shown in Fig. 9. A custom plastic casing is planned for the device in the future for esthetic reasons.

Computer Aided Analysis

The knee-loading device design, both electrical and mechanical, was analyzed with the assistance of software specific for the task. A voltage analysis was done in PSpice9, a circuit simulation

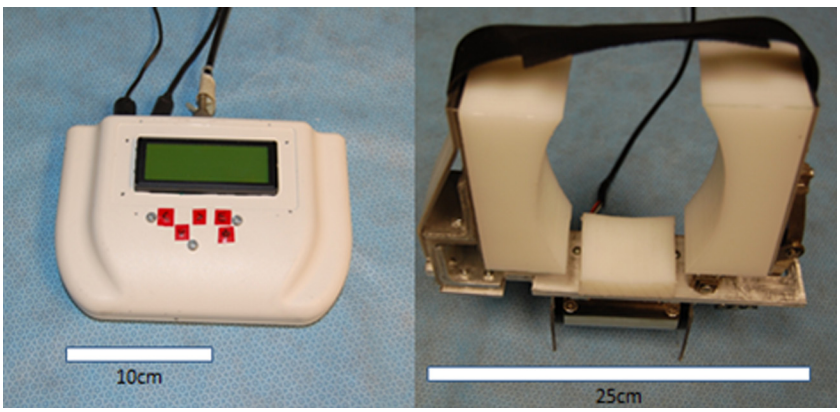

Fig. 9 (*a*) Device controller box and (*b*) as-built knee loading device

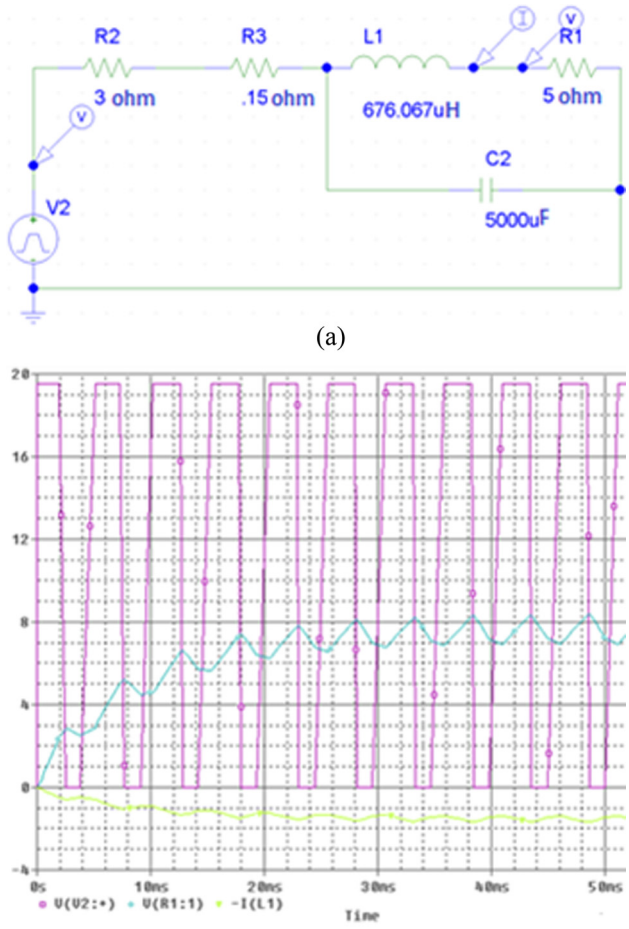

Fig. 10 (*a*) Circuit model for PSpice analysis with 200 Hz step input and (*b*) resulting voltage response across the motor

program from Cadence which is based in San Jose, CA, while a structural and modal analysis was conducted in ANSYS13, a simulation software package from ANSYS, Inc. based in Canonsburg, PA.

PSpice Circuit Analysis. A basic circuit analysis was conducted with PSpice to determine and prove the correct capacitor sizing for the PWM operating frequency of 200 Hz. The amplifier circuit was modeled in the ON position with the voltage source modeled to toggle every 5.12 ms. The modeled circuit is shown in Fig. 10(*a*). The response is shown in Fig. 10(*b*). As can be seen from the graph, the system rises within 40 ms. Some oscillation occurs in response to the PWM signal but the amplitude is small and within a usable range. Technical information about PSpice and its applications can be found in Ref. [15].

FEA Analysis. There were two different types of analyses modeled through ANSYS, static analysis and a modal analysis. For the static analysis, the maximum allowable loading conditions that could be seen for the device were applied to assure that the stress levels and deflections were within acceptable ranges for the application. The modal analysis was performed to determine the natural frequency of the assembly. This is important since it is critical to ensure that there are no loading settings that would produce frequencies near the natural frequency of the device. The model from Pro/Engineer was imported to ANSYS for the analysis. Information on the details of finite element analysis and ANSYS can be found in Ref. [16].

Static Load Results. For the static loading, a 6.9 kPa pressure is evenly distributed across the 64.5 cm^2 surface of both side of the pads directed outwards. A 44.5 N force is applied to the center of the motor shaft pushing away from the motor. This loading simulates the force applied by the motor and the reaction on the pads from the knee being loaded. The model with the loading is shown in Fig. 11(*a*). From Fig. 11(*b*), it can be seen that the maximum stress levels of the knee loading device are below the yield stress of components.

The areas of highest stress concentration are found in the base plate of the device. The maximum stress calculated along the base plate is 25.2 MPa. This gives the device a 9.5 factor of safety as the yield strength of the 6061 alloy T6511 temper aluminum used in the base plate is approximately 241 MPa. The factor of safety in steel lever arm is even higher since the stress is lower and the yield strength is higher (379 MPa for the O1 tool steel used). The next characteristic of the static analysis to consider is the total deflection of the arms as they apply the load to the patient's knee. The maximum deflection of the arm of the device was found in the static load analysis to be 8.07 mm. However, this deflection takes place in the upper section of the application arm as can be visually seen in Fig. 11(*b*), and it is important to consider that the majority of the support to the knee will take place in the middle portion of the application arm. This section only deforms 0.54 mm, which corresponds to 6.7% of the maximum axial motion of the lever arm, an acceptable amount for this application.

Modal Analysis Results. Modal analysis provides valuable information about the dynamic response characteristics of the knee loading device. This information provided by this analysis includes the natural frequencies and mode shapes of the simple and outer geometry shapes at room temperature. This serves to determine the viability of the design and the level of noise and vibration that can be expected. The basic criteria which determine the dynamic response levels are the proximity of the operating frequency to resonance, excitability of the mode, and force and damping levels. Information regarding the computation of natural frequencies and system responses can be found in Ref. [17].

From the modal finite element analysis, the first modal frequency was not found to occur until almost 62 Hz. This is well above the maximum operating loading frequency of 20 Hz.

Experimental Setup

Two types of experiments were run in this study. The first set of experiments was made in order to characterize the force applied by the device for the different motor and loading frequencies. For these experiments, the setup consisted of the device without the polyethylene pads. A solid steel bar that stretched from one supporting side to the other was placed in the loader. This steel bar was set on an aluminum block of sufficient width to provide stability. A load cell was placed directly on the end of the steel plate in direct contact with the aluminum side plate on the side of the device with the mechanism.

Once the device was successfully characterized, an experiment was performed using an artificial knee. The knee used was made of polymers and included both artificial flesh and artificial bone inside. The aim of the test is to show the viability of the device and provide an example of tests that could run with real human knees for research during a clinical trial. The setup of the experiment placed the fake knee in the device while a linear displacement sensor measured the displacement of the knee and a load cell measured the force applied to the knee. Figure 12 shows an image of this setup.

A dSPACE real-time rapid prototyping controller called MicroAutobox II (ACE MABX II) from dSPACE, Inc., Paderborn, Germany was used to record the measured displacement values. The force data was recorded using software from the load cell manufacturer Futek. Data recording was meant to be

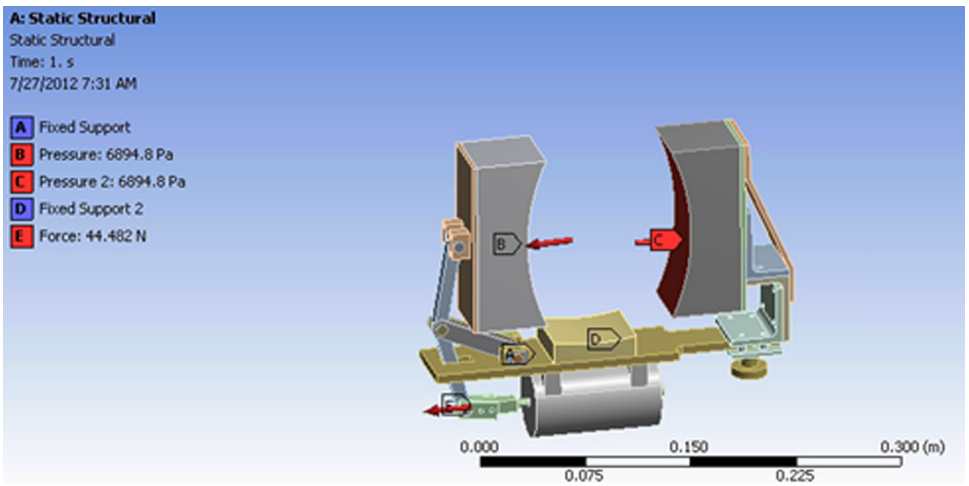

(a)

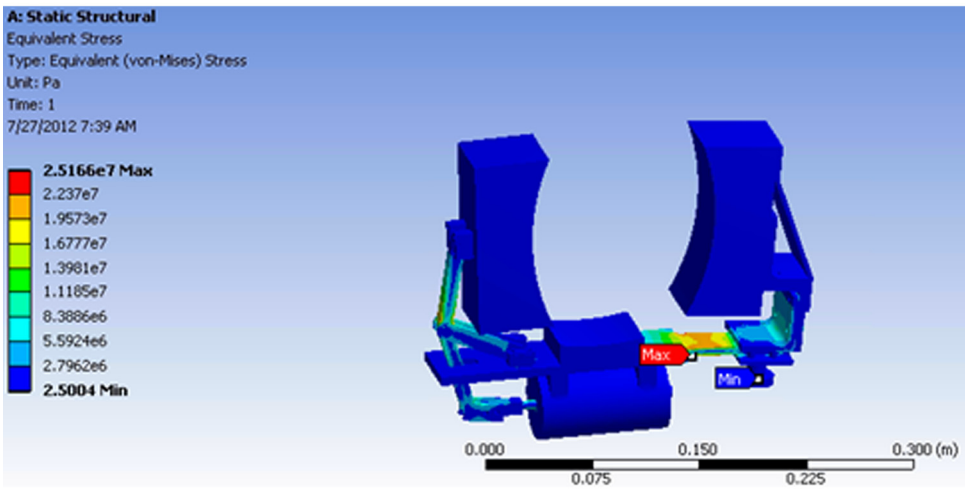

(b)

Fig. 11 (*a*) Loading and constraints of ANSYS analysis (*b*) Von-Mises stress analysis

synchronized; so both the dSPACE and the Futek program were started simultaneously. A sampling rate of 1 kHz was used for the collection of the load and displacement values. Because the programs were started manually, some human error was introduced in the synchronization. The data curves shown in the results section had to be matched as closely as possible manually. This likely introduced some error as it is possible that a very slight phase shift may exist due to energy absorption by the plastics in the fake

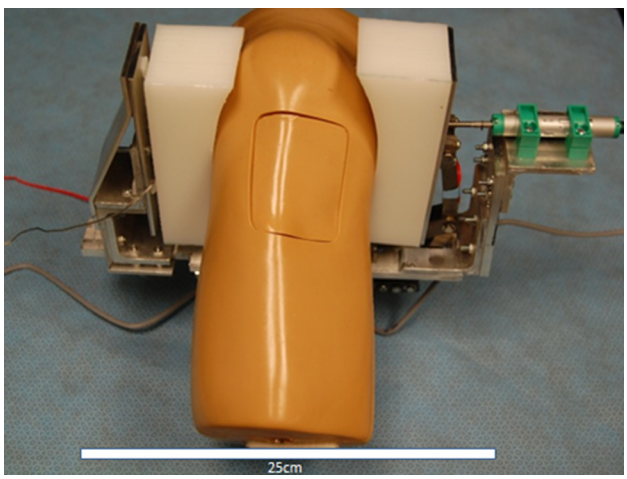

Fig. 12 Device setup for displacement and force measurements using an artificial knee

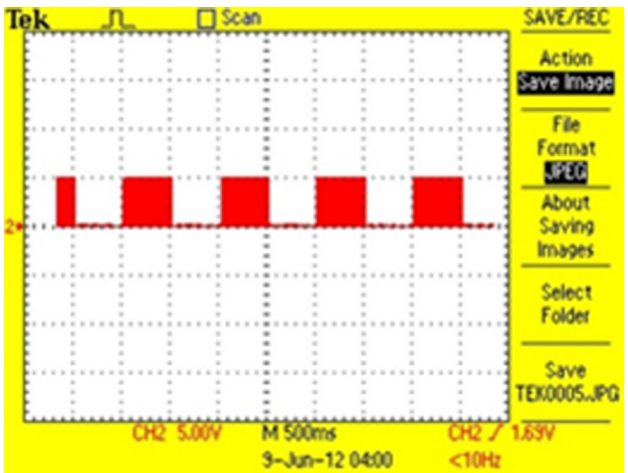

Fig. 13 Microcontroller output at 1 Hz loading frequency and 50% PWM duty cycle

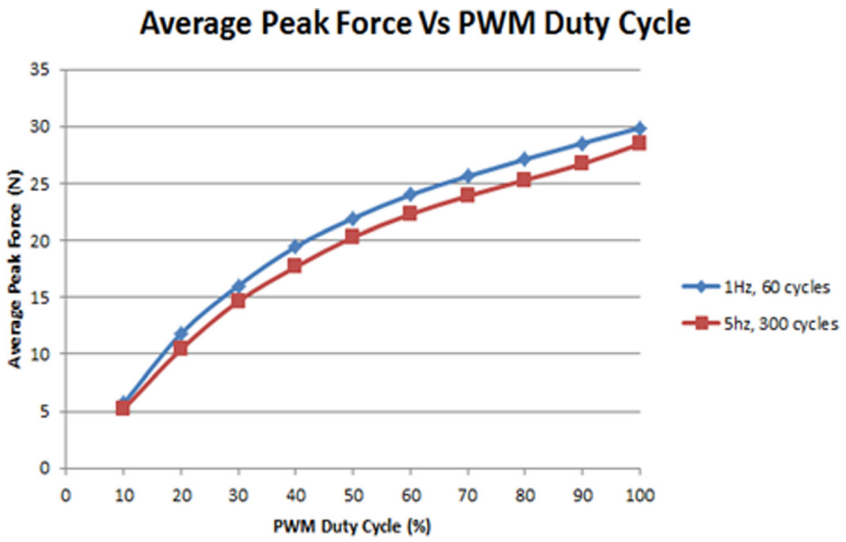

(a)

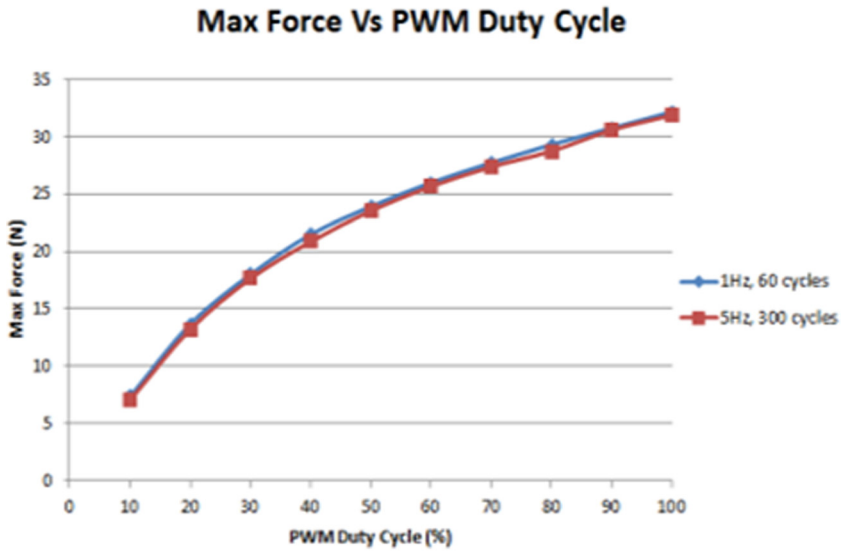

(b)

Fig. 14 (*a*) Average peak force measured over 1 min of operation at 1 and 5 Hz. (*b*) Maximum peak force occurrence measured over 1 min of operation at 1 and 5 Hz.

knee; this real phase shift, if it exists, would be eliminated when the data was manually synchronized. To allow perfect data synchronization, future tests will be conducted with a load a cell compatible with dSPACE.

Results

Once the device was fabricated as designed, several tests were run to ensure the device operated as anticipated and to simulate possible experiments that could potentially be conducted during a clinical trial. The first test that was run was a simple voltage reading of the signal produced by the controller. While basic, it was necessary to affirm that the electrical system was outputting at the correct frequencies, both PWM and loading. Figure 13 shows the output from the microcontroller at 50% duty cycle and a 1 Hz loading frequency.

As can be seen in Fig. 13, the microcontroller output is exactly what it should be. After the controller signal was verified, the force that was transmitted through the mechanism was directly measured with a load cell. The force was measured at multiple loading frequencies and PWM duty cycles. The force outputted by the motor was found to not be a perfectly linear function of the duty cycle. Figure 14(*a*) shows the average peak force transmitted through the mechanism versus the PWM duty cycle. The average was taken over 1 min of continuous operation. Figure 14(*b*) shows the maximum force reading that occurred during the same period. As can be seen from these figures, the maximum force did not significantly vary with the frequency; the average force, however, was found to decrease slightly with increasing frequency. This is side effect of the large capacitor in parallel with the motor that is used to eliminate noise. The effect is small, particularly over the range of loading frequencies of most interest to the planned studies (1–5 Hz).

Once the device was successfully characterized, an experiment was performed using an artificial knee. Figure 15 shows the force and corresponding displacement over a period of five cycles at duty cycles of 50% and duty cycles of 100%. Such experiments when performed on an actual knee could be used to assist in the

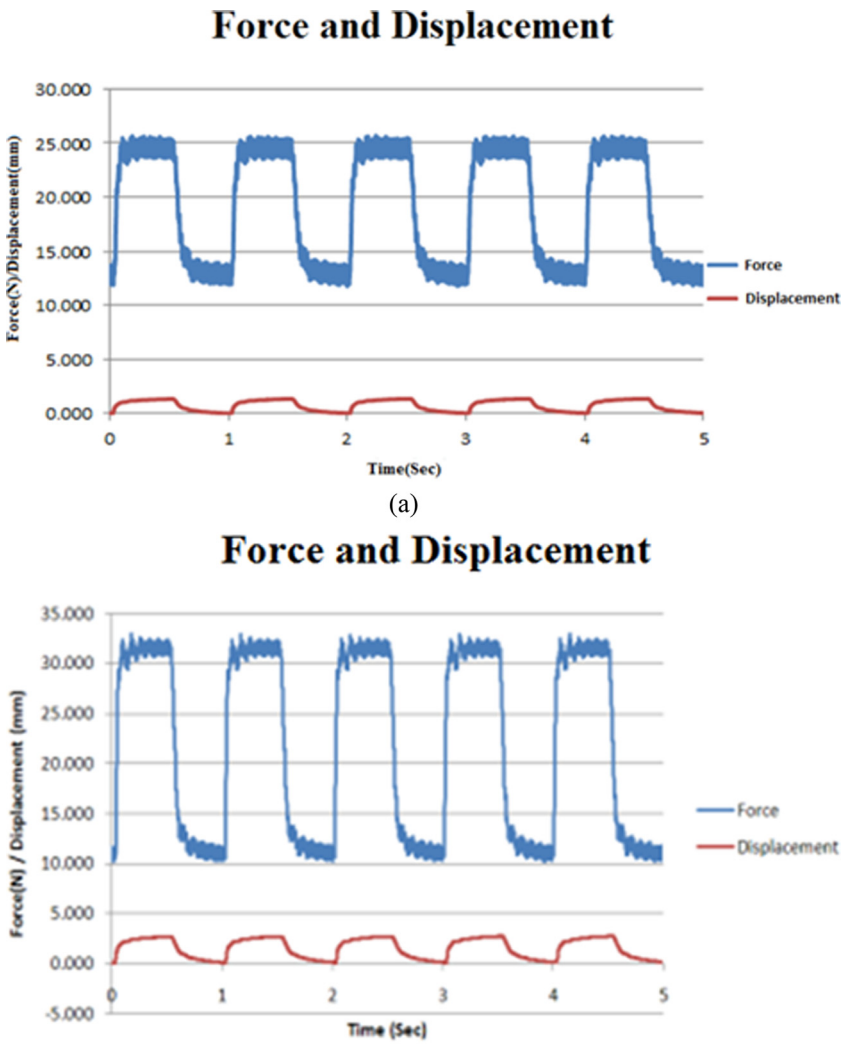

Fig. 15 Force and displacement data for an artificial knee loaded at 1 Hz and (*a*) 50% duty cycle and (*b*) 100% duty cycle

study of the force versus displacement of human tissue, a highly nonlinear reaction, as well as the effects of light mechanical loading to the bone tissue.

Conclusions

The proposed device has been designed to fulfill the voltage, weight, frequency, and other constraints. The device is made mostly of aluminum components with some steel components for the mechanism. The electrical response to the controller input was predicted in PSpice and found to be reasonably smooth. The deformed geometry, stress distribution, and modal frequencies, were analyzed with ANSYS workbench and found to be well within acceptable ranges.

The device was characterized for different loading frequencies and pulse width modulation duty cycles. While the motor response to increased power is not perfectly linear, the measured values for force will allow selection of proper duty cycles for desired forces. Tests were run with an artificial knee that demonstrated the capability of the device to be used as a means of collecting various types of data for future experiments. This device will soon be ready for submission for clinical trial, and shows promise as both a means for rehabilitation and strengthening of bone in a safe and easy manner.

Acknowledgment

This work was supported in part by an IUPUI scholarship (D.F.) and NIH R01AR052144 (H.Y.). Special thanks to Andrew Rophie and Mina Wanis of the Department of Biomedical Engineering at IUPUI for technical assistance.

References

[1] Zhang, P., Hamamura, K., Yokota, H., and Malacinski, G. M., 2009, "Potential Applications of Pulsating Joint Loading in Sports Medicine," Exerc. Sports Sci. Rev., **37**(1), pp. 52–56.
[2] Zhang, P., Malacinski, G. M., and Yokota, H., 2008, "Joint Loading Modality: Its Application to Bone Formation and Fracture Healing," Br. J. Sports Med., **42**, pp. 556–560.
[3] Zhang, P., Sun, Q., Turner, C. H., and Yokota, H., 2007, "Knee Loading Accelerates Bone Healing in Mice," J. Bone Miner. Res., **22**, pp. 1979–1987.
[4] Su, M., Jiang, H., Zhang, P., Liu, Y., Wang, E., Hsu, A., and Yokota, H., 2006, "Knee-Loading Modality Drives Molecular Transport in Mouse Femur," Ann. Biomed. Eng., **34**(10), pp. 1600–1606.
[5] Zhang, P., Su, M., Liu, Y., Hsu, A., and Yokota, H., 2007, "Knee Loading Dynamically Alters Intramedullary Pressure in Mouse Femora," Bone, **40**, pp. 538–543.
[6] Kwon, R. Y., Meays, D. R., Tang, W. J., and Frangos, J. A., 2010, "Microfluidic Enhancement of Intramedullary Pressure Increases Interstitial Fluid Flow and Inhibits Bone Loss in Hind Limb Suspended Mice," J. Bone Miner. Res., **25**, pp. 1798–1807.

[7] Zhang, P., Turner, C. H., and Yokota, H., 2009, "Joint Loading-Driven Bone Formation and Signaling Pathways Predicted From Genome-Wide Expression Profiles," Bone, **44**, pp. 989–998.
[8] Smith & Nephew Corporate, 2011, "Ultrasound Bone Healing System," http://global.smith-nephew.com/master
[9] Orthofix Inc., "Physio-Stim," 2010, http://us.orthofix.com/products/physio-stim_biobonegrowth.asp?cid=42
[10] Anthem Inc., 2012, "Electrical Bone Growth Stimulation," DME. 00004. 10/2012/2011, Anthem Medical Policy, June 21, 2012, http://www.anthem.-com/medicalpolicies/policies/mp_pw_a050280.htm
[11] Anthem Inc., 2012, "Ultrasound Bone Growth Stimulation," DME. 00004. 10/12/2011, Anthem Medical Policy, June 21, 2012, http://www.anthem.com/medicalpolicies/policies/mp_pw_a050287.htm
[12] Waldron, K. J., and Kinzel, G. L., 2004, *Kinematics, Dynamics, and Design of Machinery*, 2nd ed., John Wiley & Sons, Hoboken, NJ.
[13] Freescale Semiconductor, 2005, Mc9s12e128 Data Sheet, http://www.freescale.com/files/microcontrollers/doc/data_sheet/MC9S12E128V1.pdf
[14] ShenzenTopway Technology, Inc., 2005, "Lmb204bdc LCD User Manual," http://www.topwaydisplay.com/Pub/Manual/LMB204BDC-Manual-Rev0.1.pdf
[15] Department of Electrical and Systems Engineering, PENN, 2006, Pspice primer, "University of Pennsylvania," http://www.seas.upenn.edu/∼jan/spice/PSpicePrimer.pdf
[16] Moaveni, S., 2008, *Finite Element Analysis: Theory and Application With* ANSYS, 3rd ed., Pearson Prentice Hall, Upper Saddle River, NJ.
[17] Ogata, K., 2004, *System Dynamics*, 4th ed., Pearson Prentice Hall, Upper Saddle River, NJ.